

Article

A Boron-Containing Analogue of Acetaminophen Induces Analgesic Effect in Hot Plate Test and Limited Hepatotoxicity

Melvin Nadir Rosalez^{1,2}, Eunice D. Farfán-García³, Jesús Badillo-Romero⁴, Ricardo Iván Córdova-Chávez¹, José G. Trujillo-Ferrara³ , José A. Morales-González⁵ , Marvin A. Soriano-Ursúa^{1,*}  and Marlet Martínez-Archundia^{2,*}

- ¹ Academy of Physiology & Postgraduate and Research Section, Escuela Superior de Medicina, Instituto Politécnico Nacional, Plan de San Luis and Diaz Miron S/N, Mexico City 11340, Mexico; nadir_rosalez@hotmail.com (M.N.R.)
 - ² Laboratory for the Design and Development of New Drugs and Biotechnological Innovation, Postgraduate and Research Section, Escuela Superior de Medicina, Instituto Politécnico Nacional, Plan de San Luis and Diaz Miron S/N, Mexico City 11340, Mexico
 - ³ Academy of Biochemistry & Postgraduate and Research Section, Escuela Superior de Medicina, Instituto Politécnico Nacional, Plan de San Luis and Diaz Miron S/N, Mexico City 11340, Mexico; efarfang@ipn.mx (E.D.F.-G.); jtrujillo@ipn.mx (J.G.T.-F.)
 - ⁴ Department of Anatomical Pathology, Hospital General de Zona 2A, Troncoso. Añil 144, Granjas México, Iztacalco, Mexico City 08400, Mexico; jesus_badillo_793@yahoo.com
 - ⁵ Laboratorio de Medicina de Conservación, Escuela Superior de Medicina, Instituto Politécnico Nacional, Plan de San Luis and Diaz Miron S/N, Mexico City 11340, Mexico
- * Correspondence: msoriano@ipn.mx (M.A.S.-U.); mtmartineza@ipn.mx (M.M.-A.); Tel.: +52-55 57296000 (ext. 62751) (M.A.S.-U.); +52-55 57296000 (ext. 62782) (M.M.-A.)



Citation: Rosalez, M.N.; Farfán-García, E.D.; Badillo-Romero, J.; Córdova-Chávez, R.I.; Trujillo-Ferrara, J.G.; Morales-González, J.A.; Soriano-Ursúa, M.A.; Martínez-Archundia, M. A Boron-Containing Analogue of Acetaminophen Induces Analgesic Effect in Hot Plate Test and Limited Hepatotoxicity. *Inorganics* **2023**, *11*, 261. <https://doi.org/10.3390/inorganics11060261>

Academic Editors:
Jean-François Halet and
Gilles Alcaraz

Received: 22 May 2023
Revised: 15 June 2023
Accepted: 18 June 2023
Published: 20 June 2023



Copyright: © 2023 by the authors. Licensee MDPI, Basel, Switzerland. This article is an open access article distributed under the terms and conditions of the Creative Commons Attribution (CC BY) license (<https://creativecommons.org/licenses/by/4.0/>).

Abstract: Acetaminophen is the most sold drug to treat pain. The TRPV1 channel is among its main targets. Due to its over-the-counter availability, its use is known as the main cause of acute liver failure induced by drugs. In addition, boron-containing compounds (BCC) have shown higher efficiency, potency, and affinity than their carbon counterparts. The present study explored the potential analgesic effect and hepatotoxicity of a BCC with a similar chemical structure to acetaminophen. Docking studies were carried out on the TRPV1 channel. In addition, a hot plate test was carried out with three doses of acetaminophen (APAP) and equimolar doses of 4-acetamidophenylboronic acid (4APB) in C57bl/6 mice. These same mice were submitted to a partial hepatectomy and continued compound administration, then they were sacrificed at day seven of treatment to analyze the liver histology and blood chemistry markers. From the *in silico* assays, it was observed that APAP and 4APB shared interactions with key residues, but 4APB showed a higher affinity on the orthosteric site. Mice administered with 4APB showed a higher latency time than those administered with their equimolar dose of APAP and the control group, with no motor pathway affected. The 4APB groups did not show an increase in hepatic enzyme activity while the APAP did show an increase in activity that was dose-dependent. Although all the experimental groups did show necrosis and inflammation, all APAP groups showed a greater cellular damage than their 4APB counterparts. In addition, the LD₅₀ of 4APB is 409 mg/kg (against APAP-LD₅₀ of 338 mg/kg). Thus, in the current evaluation, 4APB was a better analgesic and safer than APAP.

Keywords: acetaminophen; boron; pain; analgesia; TRPV; hepatotoxicity

1. Introduction

Pain is an unpleasant sensory and emotional experience associated with actual or potential tissue damage [1]. The physiology of pain is a very complex process with nociceptors located on the periphery, which send signals to the central nervous system (CNS) to process those pain signals [2,3]. One of these receptors is the transient receptor potential vanilloid channel 1 (TRPV1), which is a non-selective, transmembrane cation channel that

can be activated by an array of substances related to spiciness detection and an increase in temperature related to cellular damage. Its orthosteric site is named the vanilloid pocket, but various allosteric sites have been reported [4–7]. Once it is activated, it causes a depolarization of the free nerve endings, initiating the ascending nociceptive signal, which reaches the spinal cord and travels through the ventrolateral tract to several parts in the CNS, including the cerebral cortex [8]. In contrast, it has been shown that the central activation of TRPV1 in the periaqueductal gray area can cause a series of descending noradrenergic and serotonergic pathways related to the descending antinociceptive pathway, activating alpha 2 metabotropic G0 receptors in the spinal cord and the former activating interneurons secreting GABA to inhibit the ascending nociceptive signal [3,9–13].

Acetaminophen (APAP) is the most sold over-the-counter drug to treat all types of pain. It usually tends to be overused, leading to toxic levels [14,15]. These toxic levels have led to APAP being the main cause of acute liver injury in the world, linked to its metabolism mainly occurring in the liver [15]. This toxicity has been widely related to the formation of the highly reactive metabolite, N-acetyl-p-benzoquinone imine (NAPQI), through the metabolism of APAP by the cytochrome P-450 pathway, with concomitant liver glutathione store depletion, an increase in the reactive oxygen species (ROS) with cell apoptosis, and death [16–19]. However, APAP as a modulator of pain and fever continues to be highly appreciated. The main mechanism of action for modulating pain is through the deacetylation of APAP and formation of p-aminophenol; this metabolite travels to the brain and with the help of arachidonic acid and metabolism by the fatty acid amine hydrolase (FAAH), the N-arachidonoyl aminophenol (AM404) is formed, which is a weak cannabinoid agonist and highly selective TRPV1 channel activator. Thus, AM404 is considered the APAP main active metabolite [20–24].

On the other hand, liver regeneration after a partial hepatectomy has been extensively studied [25]. The accumulated knowledge let one use the partial hepatectomy as a model to evaluate the effect of hepatotoxic drugs, such as APAP. After the excision, the initiation phase immediately begins, which corresponds with the increase in urokinase plasminogen activator in the blood. Then, the proliferation and inductive phases related to the release of various growth factors, including hepatic growth factor, endothelial growth factor, transforming growth factor, and angiopoietins [26–28]. After that, the angiogenic phase begins, which includes hyperplasia of hepatocytes, cholangiocytes, Kupffer cells, and blood vessels [29–33]. The idea of adding a boron atom into the structure of different molecules is very appealing for a drug design due to some studies having shown that boron compounds have a higher affinity, efficacy, and potency than their carbon counterparts. In addition, the body does not have the ability to break down boron–carbon bonds [34,35]. In this study, the compound (4-acetamidophenyl)boronic acid (4APB, also named 4-Acetylaminophenylboronic acid or p-(acetyl-amino)phenylboronic acid), which shares a similar structure to acetaminophen (Figure 1), was assessed to measure its ability to act as an analgesic as well as evaluate its hepatotoxicity.

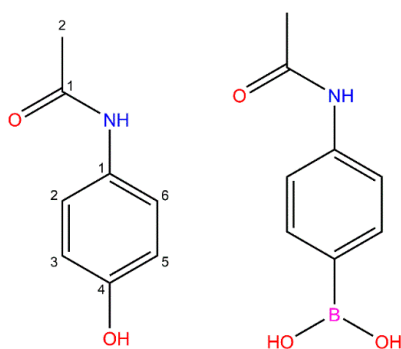


Figure 1. Chemical structures. The structures of acetaminophen (APAP, also known as paracetamol, 4-Acetamidophenol, N-(4-Hydroxyphenyl)acetamide; on the left) and 4-acetamidophenylboronic acid (4APB, on the right).

2. Results

2.1. Docking Assays and In Silico Kinetic Evaluation

Among studied compounds (see list on Table S2), compounds AM404 and AM404B (N-arachidonoyl-4-aminophenylboronic acid; boronic analogue to AM404) are notable since these metabolites of APAP and 4APB, respectively, showed a putative ability to bind with a high affinity on the TRPV1 channel.

They were predicted as high affinity ligands of both rat and human TRPV1 in the highest affinity complexes and in the second position reached on these receptors. As can be seen in Figure 2, both compounds (as well as APAP and 4APB) show higher energy values than well-known ligands, such as capsaizepine, and even higher than those for APAP and 4APB. The common interactions were hydrophobic ones, and some also related to the aromatic ring shared for all compounds. Nevertheless, the main difference between BCC and those without a boron-atom was the ability to generate additional interactions due to the existence to two hydroxyl moieties bound to the boron atom in BCC while just one hydroxyl group with ability to form hydrogen bonds in the boron-free analogues (Figures 3 and S2). Additionally, the calculated LogP and BBB prediction (as seen in Figures S3 and S4) supported the notion that these compounds could reach the CNS.

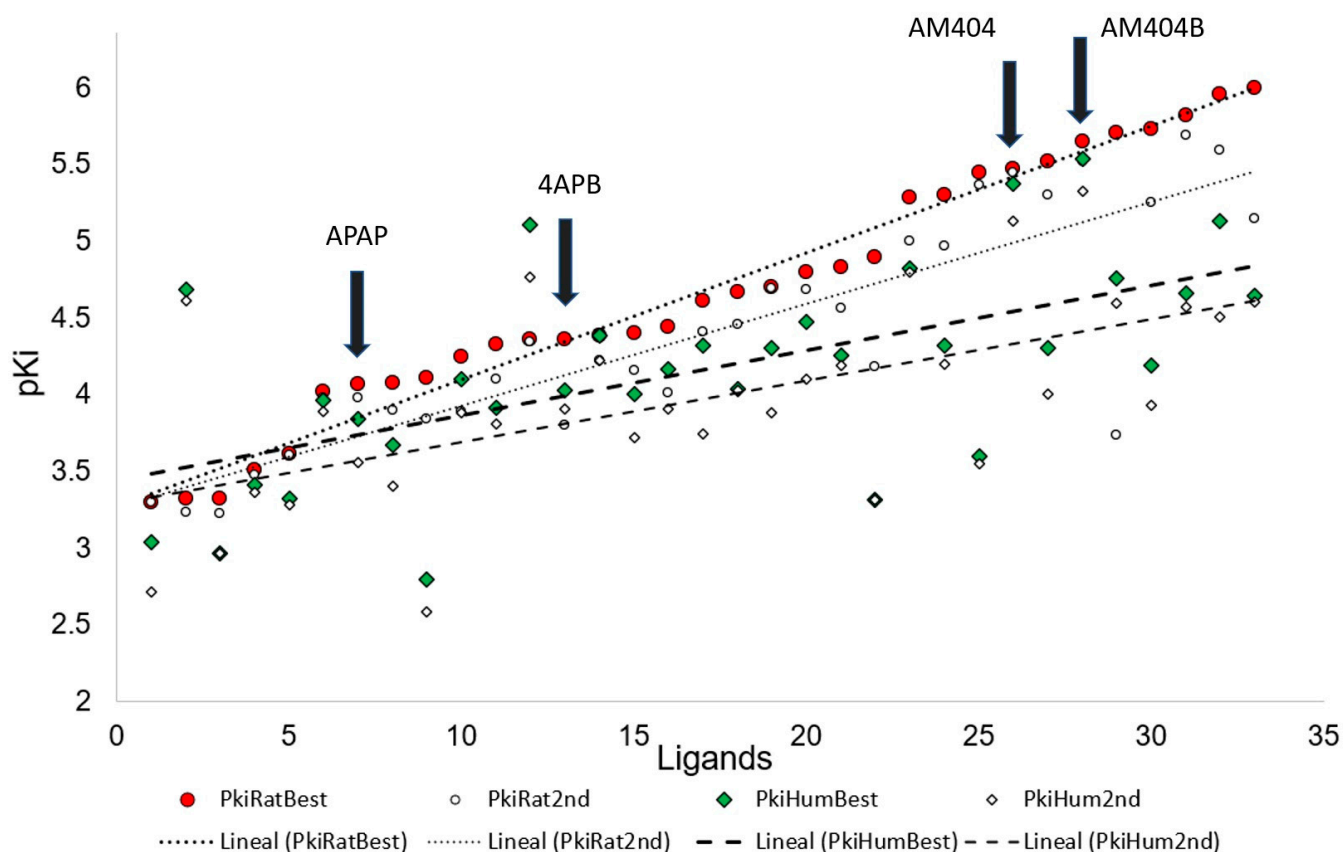


Figure 2. Predicted affinity of compounds on the TRPV1 channel. Comparison between Ki of best clusters (Filled forms) of rat (Circles) and human (Rhombs) on the TRPV1 channel; and Ki of the second best cluster (Blank forms) on the TRPV1 channel.

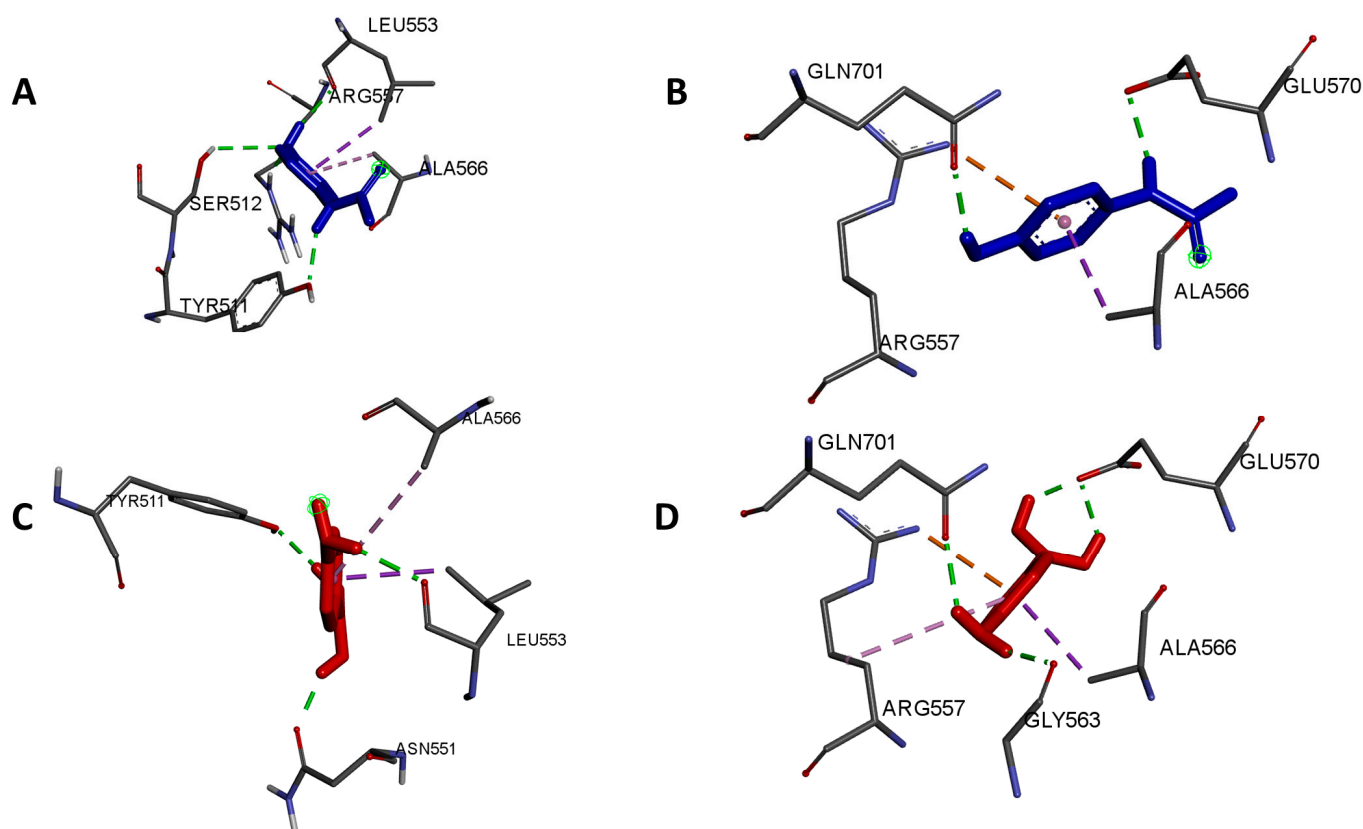


Figure 3. Predicted binding site of compounds on the TRPV1 channel. Below are APAP (A,B) and 4APB (B–D) in the orthosteric binding site. Details of interactions are in Supplementary Materials.

2.2. Determination of Intraperitoneal LD₅₀ of 4APB and In Silico Toxicity Prediction

With regards to the lethal dose 50 (LD₅₀) of 4APB, all animals were administered i.p. to avoid the idiosyncratic nature of the gastrointestinal absorption of each individual animal. In phase 1 (accord to Lorke's method, logarithmic scale), only those animals administered 1000 mg/kg of 4APB died in less than 5 min after administration. In phase 2 (doses between 100 and 1000 mg/kg considering the Lorke's method) [36], no mortality was reported during the observation period. After 48 h, all animals were sacrificed using cervical dislocation, and their brains, heart, lungs and liver were dissected. A linear regression was made with the data converting everything through the use of Probits ($r = 0.87$) and an LD₅₀ of 571.41 mg/kg and a significance of p with <0.001 , proving the correlation of the dosage and mortality rate (Figure 4). All organs dissected were observed, but no apparent damage was found.

From the in silico approach, the ProTox II online server from Charite University showed a prediction of an oral LD₅₀ of acetaminophen of 338 mg/kg with an accuracy of 100% and an active hepatotoxicity of 0.74; for 4APB, it showed an LD₅₀ of 409 mg/kg but a predicted accuracy of 68.07% and a predicted hepatotoxicity of 0.52 (details are in Figures S5 and S6).

2.3. Hot Plate and Motor Activity

It should be mentioned that 50, 150, and 250 mg of APAP were used for comparing with previous evaluations [37], and the equimolar doses of 4APB were applied (see details in Section 4.1).

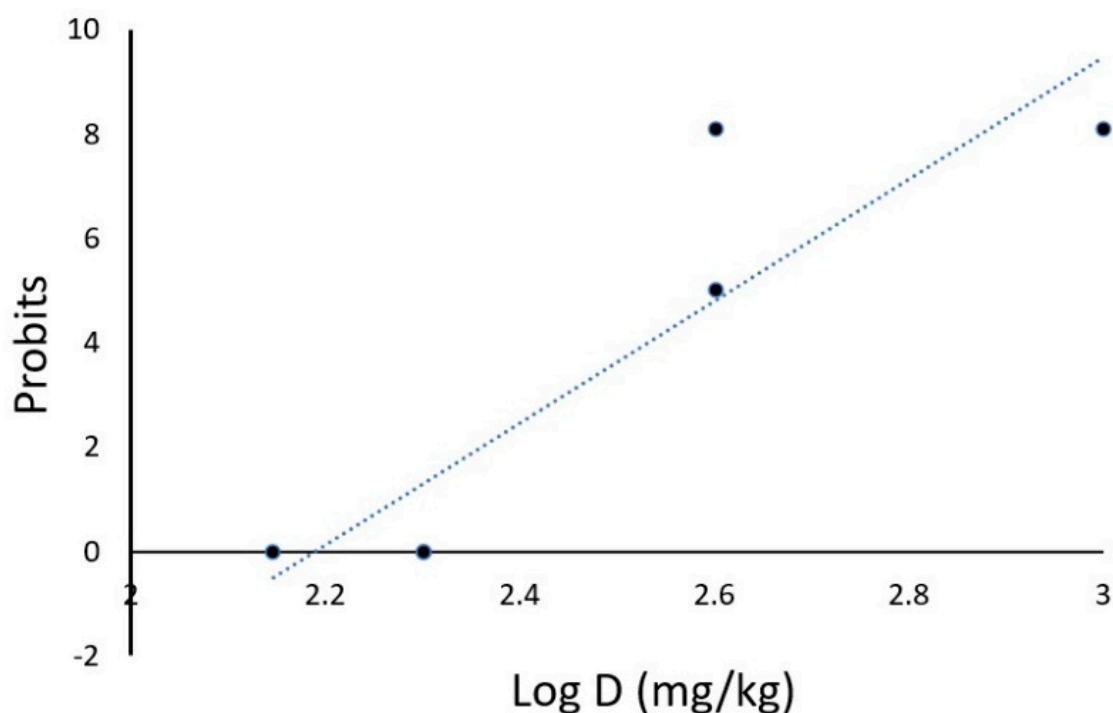


Figure 4. Quantal dose—acute toxicity response curve. Mortality in probits observed after administration of 4-APB.

For the first day of evaluation, at 30 min, 4APB150 and 4APB250 groups did show a higher latency against the control group. Higher latency values were maintained up to 120 min for these groups. Animals administered with 4APB50 showed a higher latency at 120 min. Meanwhile, APAP250 showed higher values than the control at 60, 120, and 150 min and APAP150 just at 150 min. Any statistical difference between groups was lost at 180 min (Figure 5A).

For day 2, from 0 to 90 min, all groups administered with 4APB showed a higher latency than both the control and corresponding APAP groups with a $p < 0.001$. Moreover, 4APB250 remained with a higher latency at 120 min while APAP150 showed a statistical difference at 0 and 60 min and APAP250 from 0 to 90 min comparatively to the control group. After 90 min, no statistical differences were found except for those mentioned for the 4APB250 group (Figure 5B).

On the last day, all 4APB groups showed a statistical difference with the equimolar APAP groups or control group at 0 to 150 min (except for the register at 60 min since only was difference against control group). Moreover, 4APB150 and 4APB250 groups remains with higher latency value at 180 min. For its part, APAP150 group showed higher latency than control group at 30 and 120 min while APAP250 showed higher latency than control group at 0 min (Figure 5C).

After the evaluation of motor activity, no statistical difference was observed, and no involvement of motor pathways or central or accessory pathways is suggested, as can be seen in Figure S7.

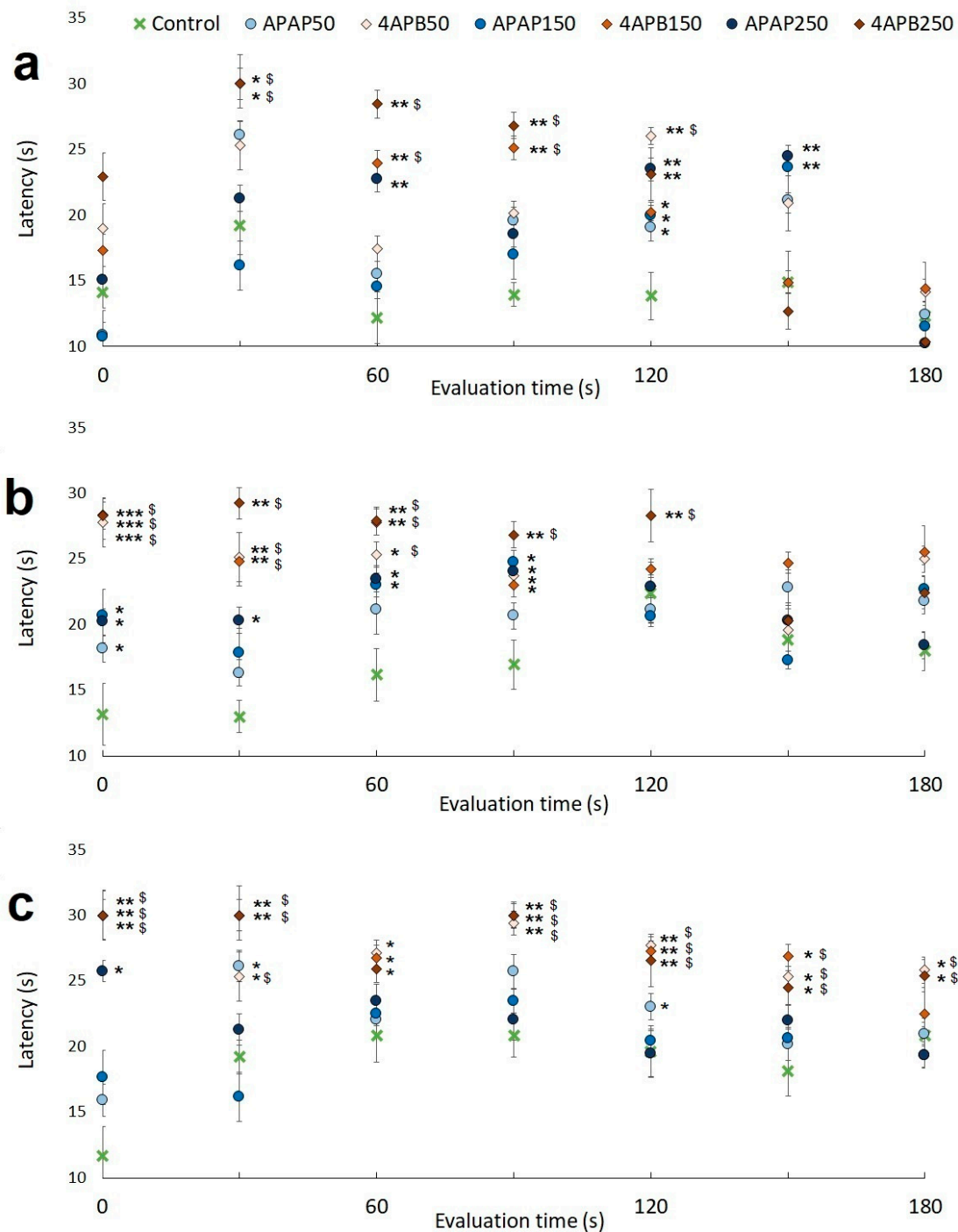


Figure 5. Latency time of mice in the hot plate test. Measured latency (in seconds) for evaluation in day 1 (a), 2 (b), and 3 (c) at 0, 30, 60, 90, 120, 150, and 180 min. Significant difference against the control group: * $p \leq 0.05$; ** $p \leq 0.01$; *** $p \leq 0.001$. Significant difference against the respective APAP group: \$ $p \leq 0.05$.

2.4. Hepatotoxicity and Liver Regeneration

Regarding hepatic metabolism evaluated by some serum metabolites, scarce differences against the control group were found (Figure 6). Thus, for glycaemia, it was established that the 4APB50 group had lower levels than the control group. For creatinine serum levels, all groups had a significantly lower concentration than the control group with a p of <0.001 . No statistical difference was found between urea, cholesterol, or albumin levels between all experimental groups and the control group.

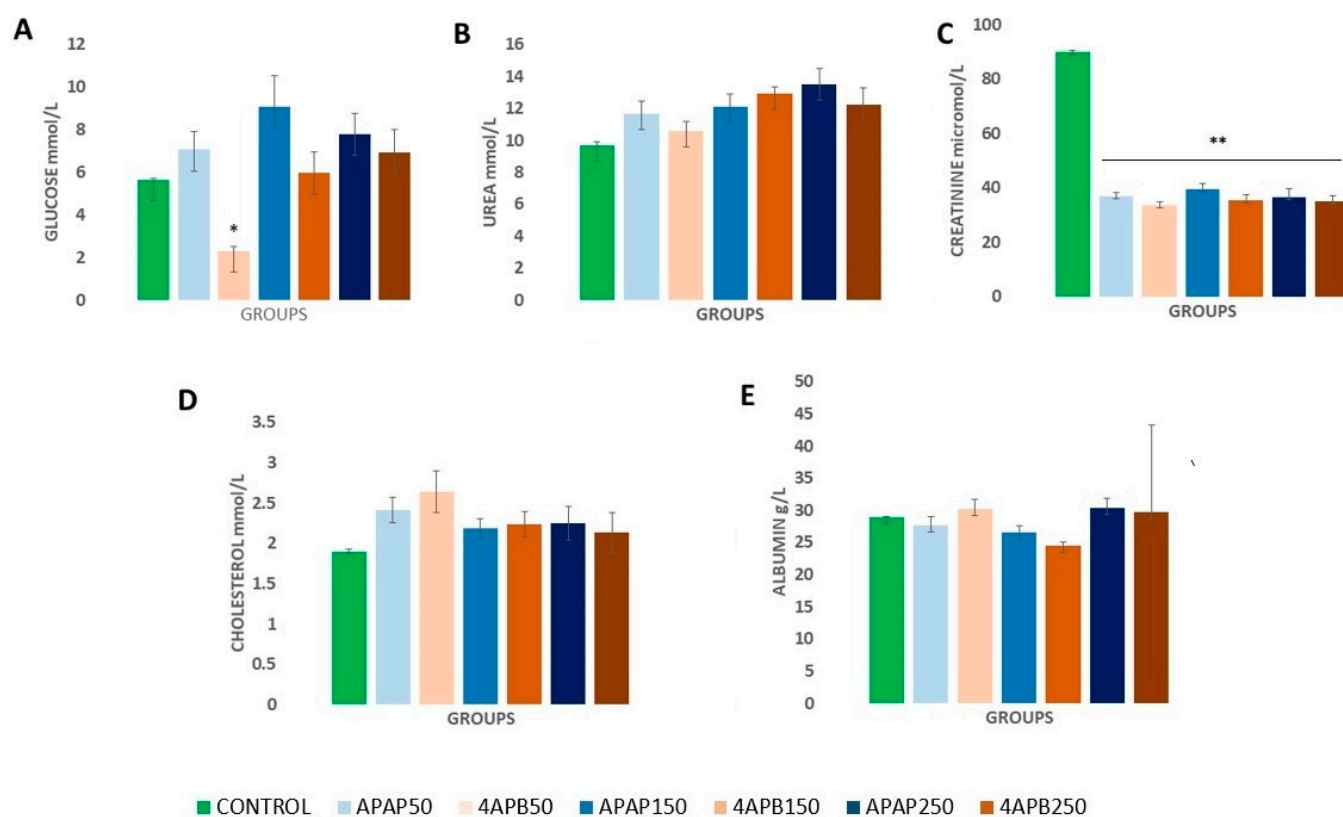


Figure 6. Serum concentrations of some hepatic metabolites. Glucose (A), urea (B), creatinine (C), cholesterol (D), and albumin (E) measured after 7 days of treatment. Asterisks indicate significant difference against control group, * $p \leq 0.05$ ** $p \leq 0.01$.

In regards to bilirubin levels (Figure 7), the APAP50 group had lower levels of total bilirubin than the control group ($p < 0.001$). As for conjugated bilirubin levels, all the APAP groups showed higher levels than the control group, and only the 4APB50 showed higher levels than the control group while all groups showed a lower level of unconjugated bilirubin compared to the control group but not between either equimolar compound group.

Regarding the activity of hepatic enzymes (Figure 8), ALT was increased in most members of the APAP groups, albeit if no statistical difference was found, while no clear pattern was found for the 4APB groups. As for AST, all groups administered with APAP showed higher levels than the control group while no statistical difference was found for the 4APB groups. For APT, no statistical difference was found among experimental groups.

With respect to the calculated hepatic regeneration, all groups did show regeneration, with the control group showing a 47.31% regeneration; APAP groups of 50, 150, and 250 mg/kg having a regeneration of 73.08%, 74.05%, and 60.95%, respectively; and the corresponding 4APB groups showing a regeneration of 49.57%, 69.36%, and 64.93% regeneration, but no statistical difference was found between any experimental group or with the control group, as shown in Figure 9.

Considering normal hepatic parenchyma and the control group as shown in Figure 10A, healthy hepatic tissue with the portal triad is present (i.e., the portal vein (PV), hepatic artery (HA), and bile duct (BD)), and although there are central veins (CV), due to the histological slice, no hepatic acinus can be discerned, but the sinusoidal spaces (SS) can be clearly demarcated. Hepatocytes (Hct) can be seen with a basophilic nucleus, with Kupffer cells (KC) having a highly basophilic nucleus with a smaller cell archetype in comparison to Hct. The effects of APAP or 4APB seem to occur in a dose-dependent manner. In Figure 10B, from group APAP50, there is a clear distinction of the healthy tissue and tissue inflammation not limited to the acinus, with a vast amount of polymorphic nuclear leucocytes, PMN; formation of fibrotic tissue, FT; fatty infiltrations, FI; and necrotic tissue,

NT. Nevertheless, as shown in Figure 10C, from the 4APB50 group, most of the samples showed healthy tissue with the presence of the normal portal triad, with no disruption of the cellular architecture or necrosis. In Figure 10D, from APAP150, there is a presence of inflammation, NT, and FT, which was more abundant than its equimolar dose of 4APB and had more HD with no distinction between the classic portal triad but a similar surface area of NT. In Figure 10E, from 4APB150 group, there is NT not limited to the acinus, diffuse inflammation, with limited inflammation and hepatocellular disorganization, HD, and the formation of FT. Finally, in Figure 10F (APAP250), there is extensive NT, various patches of FT, and diffuse inflammation with a greater surface area presentation in comparison to any other group. In the Figure 10G (4APB250), although there is NT, there are remanent Hct structures with the SS still intact with focal inflammation and the presence of FT.

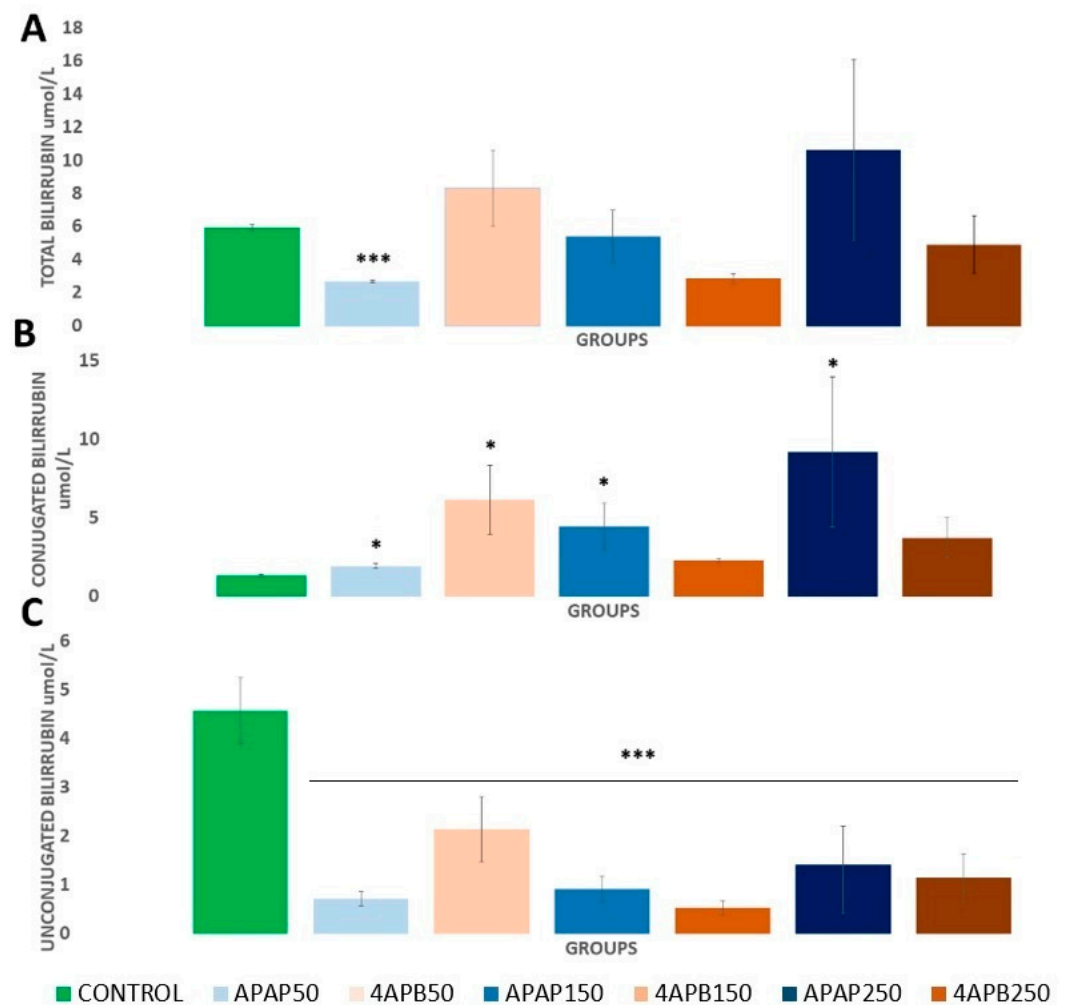


Figure 7. Serum concentrations of total (A), conjugated (B), and unconjugated (C) bilirubin. As it was measured after 7 days of treatment. Asterisks indicate significant difference against control group, * $p \leq 0.05$ *** $p \leq 0.01$.

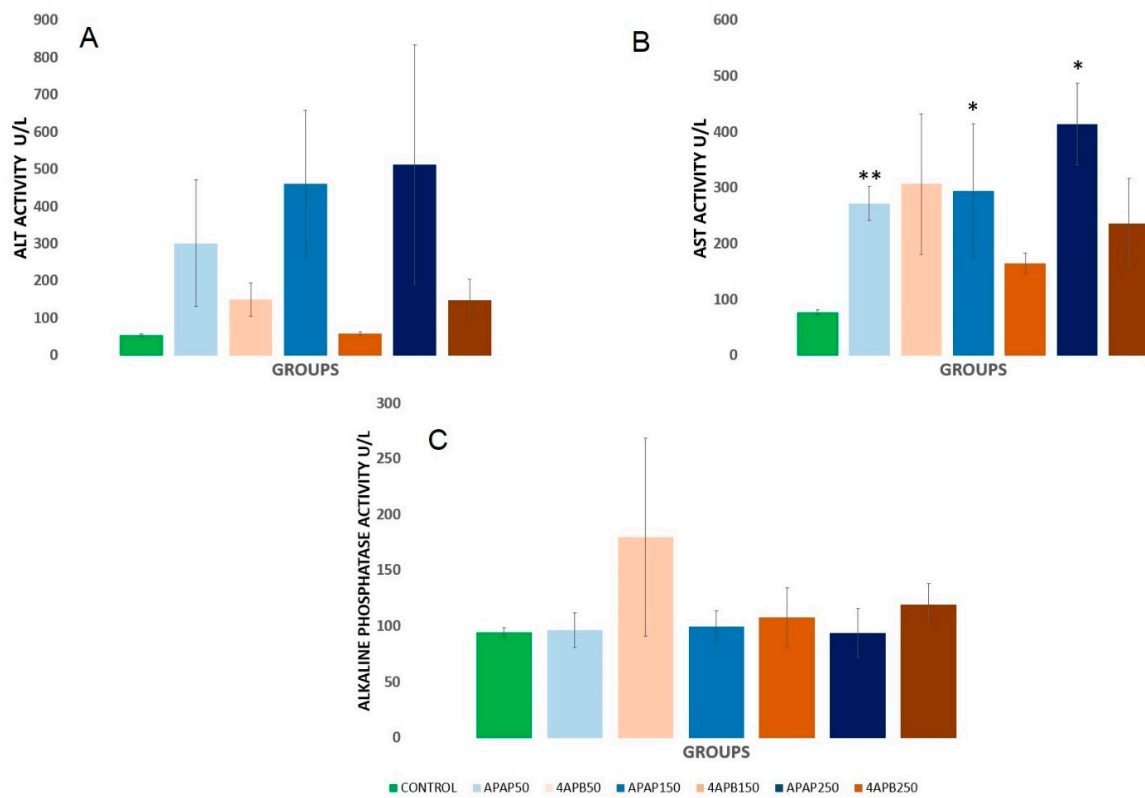


Figure 8. Serum activities of alanine transaminase (ALT, (A)), aspartate aminotransaminase (AST, (B)), and alkaline phosphatase (APT, (C)). As were determined after 7 days of treatment. Asterisks indicate significant difference against control group, * $p \leq 0.05$ ** $p \leq 0.01$.

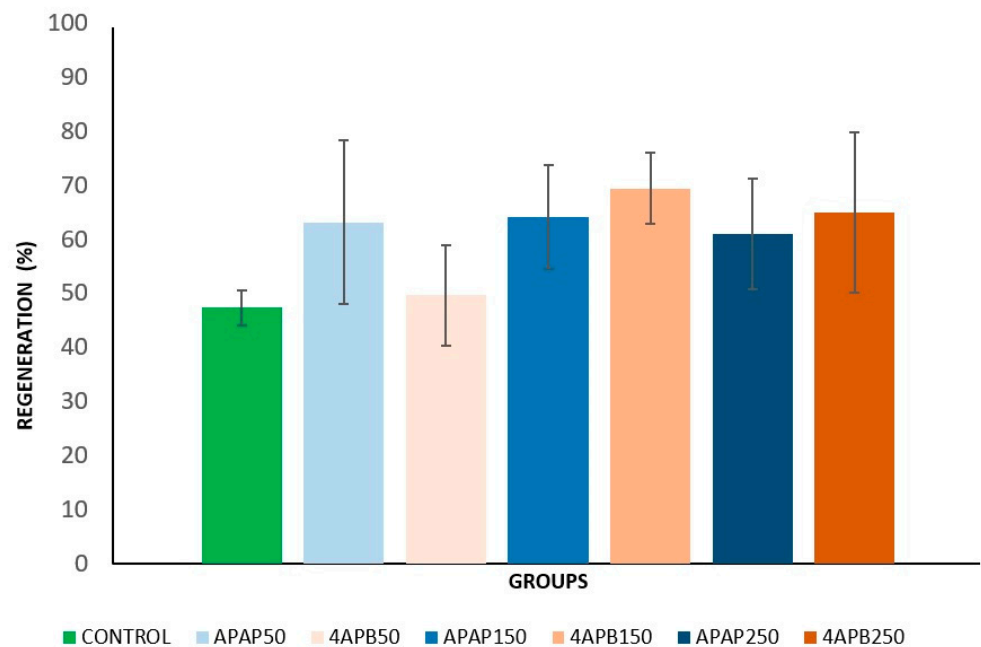


Figure 9. Percentage of mice liver regeneration after a partial hepatectomy. Percentage of regeneration determined from the final weight/expected weight relationship after 7 days of treatment. No significant differences were found among groups.

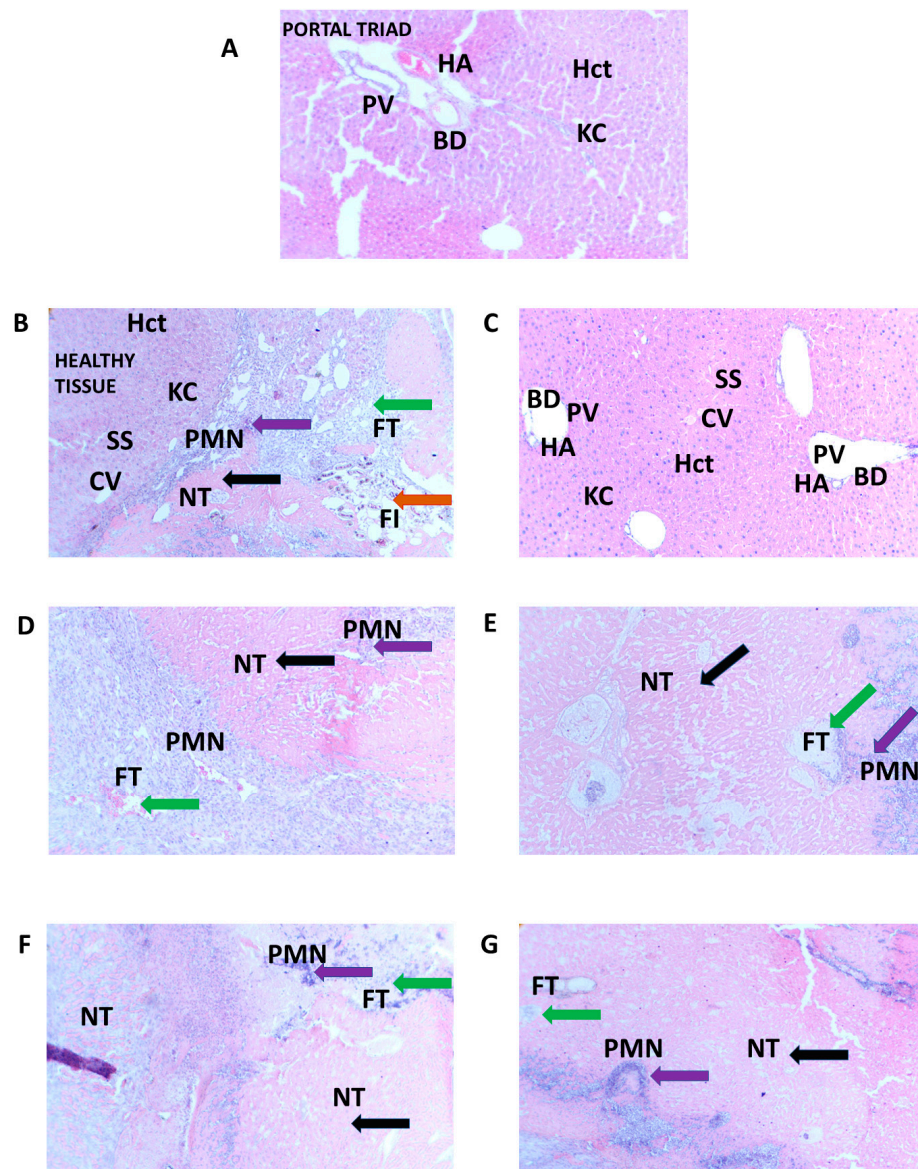


Figure 10. Hepatic Histology of samples from groups of control mice (A) or mice treated with different concentrations of APAP (B,D,F) and 4APB (C,E,G) for 7 days after a partial hepatectomy. (A) A sample from control group; a portal triad including portal vein (PV), hepatic artery (HA), and bile duct (BD) with presence of healthy hepatocytes (Hct), Kupfer cells (KC), and sinusoidal spaces (SS) are visible. (B) APAP50 with areas of loss of color and nucleus of hepatocytes with necrotic tissue (black arrow), inflammation area (purple arrow), fatty infiltration (brown arrow), and fibrotic tissue (FT) with cellular disorganization (green arrow). (C) 4APB50 and (D) APAP150 with areas of extensive inflammation (purple arrow) and hepatocellular disorganization with change to fibrotic tissue (green arrow) and necrotic areas (black arrow). (E) 4APB150 with presence of inflammation (purple arrow) with focal fibrotic tissue with hepatocellular disorganization (green arrow) and necrotic areas with loss of color and nucleus but maintaining cellular organization (black arrow). (F) From APAP250 with presence of extensive inflammation (purple arrow) with extended fibrotic tissue with hepatocellular disorganization (green arrow) and necrotic areas with loss of color and nucleus and beginning to cause hepatocellular disorganization (black arrow). (G) From 4APB250, sample with areas of loss of color and nucleus of hepatocytes with necrotic tissue (NT, black arrow), inflammation area (purple arrow), and fibrotic tissue (FT) with focal cellular disorganization (green arrow) (all figures obtained through the 10× objective).

3. Discussion

Pain is the most common symptom referred by patients that seek medical care. The mechanisms for pain are multiple; thus, the regulation of the pain pathway has been widely explored and several targets identified as key for modulation. Hence, diverse molecules interacting on these targets are applied and studied to modulate pain [1]. In this work, efforts were made on the study of TRPV1, a protein receptor functioning as a homo-tetramer related to the action of some types of pain. This protein is considered a main target for APAP pain modulation through its action in the CNS [4,6]. In our docking simulation, the subunit A was used with the grid box center between Thr550 and Ser512 to explore the vanilloid pocket and near regions proposed as key for APAP action on it. Considering the aforementioned facts as well as the *in silico* results, among tested compounds, AM404 is of special interest due to its relationship with APAP's active role in the CNS [22], and its boron-containing analogue AM404B is similarly of interest since both are theoretically BBB permeable, and thus, they can reach the CNS. Moreover, AM404 formation is enhanced through the immune system's reaction towards infections, forming a large side chain compound with putative action in CNS. Due to its high similarity in structure, AM404B could also have the possibility of being obtained from a similar bio-transformation of 4APB. Further research is required to support or discard this possibility. Nevertheless, these APAP and 4APB metabolites have the ability to form alkyl interactions with the abovementioned residues (key in the vanilloid pocket) and also due to the dipole moment of their hydroxyl group, forming hydrogen bridges with either the hydrogen or oxygen seen in the boronic acid and the acetaminophen metabolite.

The *in silico* toxicity prediction using the ProTox II server from the Charite University of Medicine, which took into account over 38,000 compounds, considering their LD₅₀ values and identification of toxic moieties, has a sensitivity of 96% and specificity of 91%. For the hepatotoxicity, it uses a Drug Induced Liver Injury Dataset, DILL, considering over 800 compounds known to cause liver injury. Thus, with regards to APAP, this server predicted an oral LD₅₀ of 338 mg/kg, toxicity class 4, and being hepatotoxic with a 75% accuracy, as shown in various studies [17,37], while the reported *i.p.* administered LD₅₀ was 367 mg/kg. This difference in concentration considers the gastrointestinal system's large surface area of absorption while the peritoneum needs diffusion for absorption and a delay of 10 to 20 s through the portal vein absorption and retention in mesentery and lymph [38]. Concerning 4APB, the predicted oral LD₅₀ was 409 mg/kg, toxicity class 4, but the predicted accuracy was 68.09%. According to that, since it was less lethal at higher doses and not hepatotoxic, but it had a probability of only 0.52, there is a need for further *in vivo* experiments to assess this assumption.

Therefore, male mice of the CD1 strain were used, and the calculated LD₅₀ was 571.4132 mg/kg. A Q-Q plot was used to better display the regression. This lower 4APB-toxicity than that for APAP may be related to the suggested high stability of the boronic acid [39], causing lower concentrations of reactive metabolites, such as NAPQI, that could be toxic for the body [40]. In addition, the possible 4APB-biotransformation to water-soluble and active metabolites. The $R = 0.87$ demonstrates the relation between dose and mortality in mice, with a p of <0.001 . In addition, determining how mg per kg impacted the mortality rate (the expected mortality rate increased by 0.1854 % per mg with a p of <0.001), it supported that 4APB is less lethal than APAP. No further macroscopic data suggesting organ toxicity were found in the necropsy of these animals.

Concerning the hot plate test, the TRPV1 channel can be activated by various stimuli, and as one is temperature, it was left at 50 °C [41]. The C57bl6 strain was used due to its sensibility towards thermic tests, and it was done in 3 days to observe acute analgesia and possible bioaccumulation at different doses. As aforementioned and considering all data from days 1 to 3, it can be ascertained that all tested doses of 4APB disrupt the nociceptive pathway to produce an analgesic effect towards thermo-nociception, but they took more time to start while APAP only showed analgesia at the highest tested dose. The data from

the open field test supported that analgesic effect evaluation was not altered by motor disruption [42].

In regards to plasma metabolites or those molecules related to systemic metabolism, of special interest is glucose due to APAP being able to oxidize free phenolic hydroxyl groups on test strips or analyzers and boric, boronic acids, or fructoborate decreasing glucose levels by a mechanism as yet to be defined, though some data point to insulin-related activity [43–46]. In these results, only the 4APB50 group showed a reduction in glucose; it could be related to the effects of other BCC in carbohydrates metabolism [46].

Linked to the protein metabolism, the plasma levels of urea, a soluble metabolite produced from ammonia so as to be excreted [47], were not affected in the studied mice. Then, it can be inferred that neither APAP nor 4APB affect the urea cycle; the main way to produce alterations in its production [48,49]. For its part, creatinine in the plasma for the control group was (90 mmol/L) in the normal range while all other groups were below the normal range (<88 mmol/L), inferring that both compounds could act by antagonizing metabolic processes involving the creatinine production, such as the process mediated by the action of S-adenosyl-L-methionine: N-guanidinoacetate methyltransferase [50]. In addition, it could be related to an increased glomerular filtration rate, but additional measurements should be carried out to support this.

Cholesterol is an essential lipid that is important for cellular organization and stability while also the basis for hormones, bile, vitamin D, and oxysterols. Some BCC can reduce cholesterol levels [51], but in the present study, no correlation was found with the administered 4APB, while APAP can reduce levels under certain conditions, but it is generally accepted as not affecting levels [52–54]. The main protein produced in the liver, albumin, with multiple functions, was not altered in the control or experimental groups, thus implying that at these doses, the compounds or possible metabolites interfering with hepatocytes is not enough to cause a blockage of albumin synthesis as it has been reported in other cases [55–58]. Higher APAP or 4APB doses seem to be required to disrupt albumin production in the current murine model.

Bilirubin released from the catabolism of heme is usually glucuronated in the liver, so it can be excreted into bile. The metabolism of APAP produces a glucuronide metabolite that can be released in bile, and it can cause cholestasis due to impaired cellular secretion of bile [16,17]. In the results obtained in this study, no consistent increase or statistical difference in total, conjugated, or unconjugated bilirubin was observed in regards to the different concentrations of 4APB in comparison to the control group while for the APAP groups, there is an increase in conjugated bilirubin levels noted from the lowest dose (50 mg/kg). This could be related to the effect observed histologically in the liver tissue (acute liver damage with fibrosis, see below) and in line with cholestasis [59–62].

The enzymes AST, ALT, and APT are widely used to assess liver damage, although there is a normal serum activity due to the normal replacement of hepatic cells, and AST can be found in almost all tissues while ALT and APT in some other organs. Although no statistical difference was found between groups for ALT or APT, for ALT in the three APAP groups, there was an increase that correlated with the dose (i.e., the mean value of APAP50 was increased 4-fold from normal values, that for APAP150 group was increased 6-fold, and that for APAP250 was a 7-fold increased value. In the 4APB groups, just a slight increase is noted in mean values, suggesting lesser hepatic damage than APAP. In regard to AST, there is a statistical difference with all APAP groups against the control group with the mean value increase being dose dependent, inferring that they did cause acute liver damage [63,64]. This was not observed with 4APB. Moreover, this is in line with the results recently reported by Celyk and Aydin; they found 4-hydroxyphenylboronic acid (structurally related to the compound tested in the current work) administration to mice that decreased the elevated AST and ALT levels induced by APAP (20 mM in liver-cell culture) [65].

In addition, it should be noted that the normal weight of the liver in mice is 5% of the total body weight, and through a partial 2/3 hepatectomy, it can cause a total weight recov-

ery after 7 days from the surgery through cell hypertrophy followed by proliferation [66]. However, if hepatotoxic compounds are added, they can limit regeneration or stimulate hypertrophy [67,68]. In the present study, no statistical difference was found between the liver mass of the control group or experimental groups, but in almost all the treated groups (exception is the lowest dose of 4APB), there was an increase in the mean value of the percentage of regeneration. This is in line with the possibility of the stimuli of toxic compounds for increasing the hepatic mass due to stimulation of liver hypertrophy [66–69] or the production of some liver growth factors (as epidermal growth factor, tumor necrosis factor alpha, hepatocyte growth factor, and interleukin-6) [70]; some of these growth factors are altered by BCC administration [71].

Finally, regarding the histology, the control mice showed a normal hepatic parenchyma. The effects of APAP of 4APB administration were clearly dose-dependent; however, it was clear that higher concentrations of 4APB than APAP were required to induce morphological changes, inflammation, and fibrosis processes. In addition, necrosis was observed in increased distribution in the three tested doses of APAP but not in the lowest dose of 4APB. Then, there was hepatic damage done by both, APAP and 4APB by a mechanism as yet unknown but probably related in both cases to the formation of metabolites (as N-Acetyl-p-benzo-quinoneimine and other quinones), increasing the oxidative stress or directly damaging mitochondria as is probed by APAP [15,60]. Further research is required to explain the requirement of higher doses of 4APB and to probe the sharing mechanisms with APAP.

This work showed the analgesic potential of 4APB in a dose-dependent manner as well as the advantages on hepatotoxicity suggested by a model of hepatic regeneration; additional assays are required to test the antipyretic effect of this compound and the changes in entire neural and immune systems after its administration. In addition, the evaluation of biotransformation and hepatotoxicity in different ages or in different mammal species would be interesting, as some differences have been reported linked to differences in the biotransformation and production of cytotoxic metabolites [37,72].

4. Materials and Methods

4.1. Animals and Treatments

All experiments complied with the requirements established in the NOM-062-ZOO-1999-SAGARPA, with the ARRIVE guidelines and the guide for the use and care of laboratory animals of the National Research Council. Mice were maintained in cages (4 animals per cage) of acrylic with $43 \times 53 \times 20$ cm dimensions; they were 1 week at adaptation in a reverse light–dark cycle at room temperature in the area for behavioral assays, with water and food (Rodent Laboratory Chow 5001) ad libitum.

An amount of 56 male C57BL/6J healthy mice of 7–8 weeks of age, weighing 25 ± 2 g, acquired from the Vivarium of Universidad Autónoma del Estado de Hidalgo were used. Institutional Biosecurity Committee evaluated and approved this protocol, registered as ESM-CBS-07/03-11-2021. C57BL/6J mice were randomly assigned to seven groups ($n = 8$) with eight members each ($N = 56$). Groups were named for the administered treatment. With reference to administered drug, they were named APAP (from Sigma-Aldrich, St. Louis, MO, USA. Cat.A7085, CAS 103-90-2, purity $\geq 99\%$, M.W. 151.16 g/mol) or 4APB (from Sigma-Aldrich, St. Louis, MO, USA. Cat.565806, CAS 101251-09-6, purity $\geq 90\%$, M.W. 178.98 g/mol) while the numbers were regarding the applied dose (i.p., mg/kg); it should be mentioned that 50 (0.33 mmol), 150 (0.92 mmol), and 250 (1.65 mmol) mg were used as previously in similar evaluation to analgesic and hepatotoxic ability of APAP [37,73], and the doses of 4APB were applied as equimolar to those used for APAP (0.33 mmol = 59.2 mg/kg, 0.92 mmol = 177.6 mg/kg and 1.65 mmol = 296 mg/kg). Thus, group 1 was control; groups 2 to 4 were administered with APAP: APAP50, APAP150, APAP250; and groups 5 to 7 were those administered with the equimolar quantity, 4APB: 4APB50, 4APB150, and 4APB250. The hot plate test and hepatotoxicity (the latter one week after analgesic evaluation) were evaluated in the same mice as is explained in Sections 4.5 and 4.7.

In addition, for comparative purposes (with previous reported toxicity [37,60]), 17 CD1 male mice were used to test toxicity as is described below (see Section 4.4).

4.2. Retrieval of Tested Structures

The structures of a set of 34 ligands were drawn using ACD/ChemSketch 2020.1.2. This group included known APAP metabolites, the potential metabolites of 4APB; capsaicin, a natural vanilloid; and capsazepine, a synthetic antagonist of the TRPV1 Channel. These ligands were pre-optimized using Hyperchem, Version 6.0, Hypercube, Gainesville, FL, USA, at the level of molecular mechanics at AM1 basis set. Thus, the minimum energy structure for each ligand was fully optimized at the B3LYP/6-31G** level using Gaussian 09 software.

The structure of the rat-TRPV1 channel (PDB ID:5IRX) was selected due to the fact that this entire protein was obtained in a native bilayer environment for rat [74] while the <https://swissmodel.expasy.org> server (accessed on 20 January 2020) was used to create a human TRPV1, which represented a model based mainly on one crystal structure (PDB ID: 3j5p, a minimal functional rat TRPV1 construct, composed of amino acids 110 to 603 and 627 to 764), which had a similarity of 92.31 % to the one for the human protein [4]. Data regarding proteins structure evaluation are presented in Supplementary Materials (Figure S1 and Table S1).

4.3. Docking Procedure

The targeted protein was prepared as described above and as previously reported [75]. Autodock Tools 1.5.7 was used to prepare docking studies as elsewhere [76], a blind approach was employed to explore the vanilloid pocket and to identify or discard putative allosteric binding sites. For the search, a Lamarckian genetic algorithm was used with a population of 100 random individuals and 10×10^7 iterations, which ran with the AutoDock 4.2 software. The results were analyzed for affinity value estimation and interactions with AutoDock Tools 1.5.7, and images were obtained using Discovery Studio Visualizer v20.1.0.19295 [77].

Additionally, to determine if the molecules studied could pass the blood–brain barrier, the calculated logP or the octanol–water partition coefficient was calculated using logP (octanol–water) partition coefficient calculation (by using <https://molinspiration.com>, accessed on 16 January 2020) server to determine the hydrophobicity; a positive number being further away from 0 indicated an increase in hydrophobicity, and those that had negative values were hydrophilic. In addition, to correlate the answer, the log blood–brain barrier (BBB) Prediction Server (by using <https://cbligand.org/BBB/predictor.php>, accessed on 16 January 2020) server was used to discern if the molecule studied could pass the blood–brain barrier, which used a Support Virtual Machine (SVM) algorithm to offer a value, which, if positive and further away from log 0, meant that it could pass the barrier while a number with negative results showed that it could not pass it.

4.4. In Silico and In Vivo Toxicity Evaluation

The Pro Tox II server by the Charite University was used to infer toxic properties, and for the Query, the PubChem Code for APAP and 4APB was acquired.

The in vivo preliminary acute toxicity was determined using the Lorke's Method [36]. In brief, 17 male CD1 mice of 7–8 weeks of age and weight of 25 ± 2 g were used, with phase 1 consisting of 3 groups of 3 mice administered an intraperitoneal (i.p.) dosage of 10, 100, and 1000 mg/kg of the compound 4APB, and they were observed for 24 h for changes in behavior and mortality. Phase 2 consisted of 4 groups of CD1 male mice; 2 mice in each group with dosages of 50, 140, 200, and 400 mg/kg of 4APB; and an observation period of 24 h for changes in behavior and mortality. For the calculation of LD₅₀, a linear regression for the lethality was calculated by converting the percentage to probits [78,79].

4.5. Hot Plate Test

After one week of adaptation, the C57BL6 mice were administered their correspondent treatment (APAP or 4-APB, in days 1, 2, and 3, i.e., they were administered daily), which was a vehicle of NaCl solution at 0.9% with 10% DMSO delivered i.p. 30 min prior the hot plate test. For the test itself, the hot plate (OmniAlva[®], Mexico City, Mexico) was set at 50 °C. Every 30 min, the animals were put on the hot plate, and the latency time was measured for 3 h and for 3 days, with the time limit being 30 s to prevent tissue damage. An independent researcher was taught to read the changes in behavior for the recording in latency time, which included jumping from the base of the hot plate, moving their hind paws uncontrollably, or when they licked their front and hind paws [41].

4.6. Open Field Test

Animals were put in an acrylic box (50 × 50 × 50 cm) linked to the OmniAlva[®] Open field equipment (Mexico City, Mexico), their exploratory and freezing behavior was observed and recorded during 5 min. This occurred 1 h before any procedure to avoid animals with motor limitations and 2 h after the administration of the APAP or 4APB to measure effects of treatment on motor performance [42].

4.7. Partial Hepatectomy Model

After the hot plate test, male C57bl6 mice were given 7 days of additional adaptation and rest. For the eighth day, the surgical removal of 2/3 of the liver using a technique known as a partial hepatectomy (PH), which was performed according to the procedure described by Higgins and Anderson [80], which corresponds to the removal of the medial and lateral lobe with a single ligature of the common pedicle with a later excision of the lobes aforementioned. As a surgical control, the control group did have part of their hepatic mass removed but were administered saline solution [25,80]. For the corresponding 7 days, each group was administered daily as aforementioned. All groups received food and water ad libitum throughout the treatment period.

On day 8 after PH, animals were sacrificed through a lethal dose of sodium pentobarbital (120 mg/kg BW). Serum samples were obtained through an intracardiac puncture. Each animal was washed with a phosphate-buffered saline solution with a phosphate tampon and posteriorly with 10% formaldehyde solution. The livers were cut, weighed, and placed in a solution with 10% formaldehyde solution and put to freeze at −70 °C until later use.

To determine liver regeneration with regards to the resected liver, it was weighed and divided by 0.7 to obtain the estimate of the initial weight while for the percentage of restituted hepatic mass, the following formula was used: remnant liver weight/initial liver × 100 as elsewhere [81].

4.8. Liver Histology

Hepatic samples were fixed with formaldehyde (10% in isotonic solution), embedded in wax, and stained with hematoxylin-eosin, with the specimens read blindly without knowledge of other data by two independent expert observers. The criteria that were used to analyze the morphological abnormalities were: fatty infiltration (+ mild, ++ moderate, +++ severe, and ++++ very severe), inflammation (+ zonal localization, focal inflammatory cells, ++ moderate, not restricted to one zone of the acinus, +++ diffuse), and hepatocellular disorganization (+ isolated foci in zone 3 of the liver acinus, ++ more widespread, and +++ definitively diffused in the hepatic acini).

4.9. Determination of Enzymes and Metabolites in Serum

The activities of serum alanine aminotransferase (ALT), aspartate aminotransferase (AST), and alkaline phosphatase (APT) were measured using the colorimetric diagnostic kits (Spinreact de Mexico, SA de CV) and reported in units/L. Serum concentrations of glucose (mmol/L), cholesterol (mmol/L), urea (mmol/L), creatinine (μmol/L), albumin

(g/L), and bilirubin ($\mu\text{mol/L}$) were determined with spectrophotometric techniques using diagnostic kits (Spinreact de Mexico, SA de CV).

4.10. Statistics

Statistical analysis was carried out with Shapiro–Wilk test to verify normality in the data collected, and if the former was positive, one-way ANOVA was used while if it failed, a non-parametric test was used, such as Kruskal–Wallis test (i.e., for data from the hot plate test and open field activity, one-way ANOVA was used, and when Shapiro–Wilk test failed, Kruskal–Wallis test was used), and for post hoc tests, Tukey’s, Dunn’s, and Holm–Sidak were used. For data from in vitro assays of hepatic metabolites and enzyme activity, one-way ANOVA was used, and when Shapiro–Wilk failed, Kruskal–Wallis was used. For the comparison between individual groups, whether for the hot plate test, open field test, hepatic metabolites, and enzymes, for the mean comparison, *t*-test was used if normality was passed, or rank sum test was applied for medians. Analysis of data was performed using Sigma Plot 14.0[®]. Significance was considered when $p \leq 0.05$.

5. Conclusions

Considering the data acquired from the in silico and analgesic evaluation, it can be suggested that the vanilloid pocket of the TRPV1 channel is an important site for the action of both APAP and 4APB (and probably some of their metabolites). In addition, from these results, it could be suggested that 4APB does have an analgesic effect (in the three tested doses) towards thermal nociception while APAP has an analgesic effect at the highest tested dose only. In addition, from LD50 value, it was shown that 4APB is less toxic than APAP, and from some enzymatic and morphologic changes, it was shown that 4APB is less hepatotoxic than APAP; hence, 4APB in low doses is probably more effective as well as safer than APAP at treating pain.

Supplementary Materials: The following supporting information can be downloaded at: <https://www.mdpi.com/article/10.3390/inorganics11060261/s1>, Figure S1: Ramachandran Plots; Figure S2: 2D interaction schemes of 4APB and APAP on TRPV channels; Table S1: Results from Swiss-model server; Table S2: Evaluated compounds and their codes; Figure S3: Log values for tested compounds; Figure S4: blood brain barrier Index values predicted for tested compounds; Figure S5: ProToxII server prediction for 4APB and APAP; Figure S6: In Silico toxicity model report for 4APB and APAP; Figure S7: Results in the Open Field Test evaluation.

Author Contributions: Conceptualization, M.N.R., M.A.S.-U. and M.M.-A.; methodology, M.N.R., R.I.C.-C., E.D.F.-G. and J.B.-R.; software, M.N.R. and R.I.C.-C.; formal analysis, M.N.R., J.G.T.-F., E.D.F.-G., M.A.S.-U. and M.M.-A.; data curation, J.A.M.-G., M.A.S.-U. and M.M.-A.; writing—original draft preparation, M.N.R. and M.A.S.-U.; writing—review and editing, M.N.R., E.D.F.-G., J.A.M.-G., M.A.S.-U. and M.M.-A.; supervision, J.G.T.-F., M.A.S.-U. and M.M.-A. All authors have read and agreed to the published version of the manuscript.

Funding: The authors would like to thank the Consejo Nacional de Ciencia y Tecnología (CONACyT). In addition, the authors thank the Secretaría de Investigación y Posgrado del Instituto Politécnico Nacional for the financial support of this project (Grant: M-2143).

Data Availability Statement: Not applicable.

Acknowledgments: The authors thank Agustin Montes de Oca Acosta, from Laboratorio Experto Veterinario for helping us in the analytical assays of serum samples; the authors also thank Alexia V. Montes-Aparicio, for the helpful assistance in the in vivo evaluation assays.

Conflicts of Interest: The authors declare no conflict of interest.

References

1. Raja, S.N.; Carr, D.B.; Cohen, M.; Finnerup, N.B.; Flor, H.; Gibson, S.; Keefe, F.; Mogil, J.S.; Ringkamp, M.; Sluka, K.A. The revised IASP definition of pain: Concepts, challenges, and compromises. *Pain* **2020**, *161*, 1976. [[CrossRef](#)] [[PubMed](#)]
2. Ossipov, M.H.; Dussor, G.O.; Porreca, F. Central modulation of pain. *J. Clin. Investig.* **2010**, *120*, 3779–3787. [[CrossRef](#)]

3. Moriya, S.; Yamashita, A.; Nishi, R.; Ikoma, Y.; Yamanaka, A.; Kuwaki, T. Acute nociceptive stimuli rapidly induce the activity of serotonin and noradrenalin neurons in the brain stem of awake mice. *IBRO Rep.* **2019**, *7*, 1–9. [[CrossRef](#)]
4. Liao, M.; Cao, E.; Julius, D.; Cheng, Y. Structure of the TRPV1 ion channel determined by electron cryo-microscopy. *Nature* **2013**, *504*, 107–112. [[CrossRef](#)] [[PubMed](#)]
5. Jara-Oseguera, A.; Simon, S.A.; Rosenbaum, T. TRPV1: On the road to pain relief. *Curr. Mol. Pharmacol.* **2008**, *1*, 255–269. [[CrossRef](#)] [[PubMed](#)]
6. Brito, R.; Sheth, S.; Mukherjea, D.; Rybak, L.P.; Ramkumar, V. TRPV1: A potential drug target for treating various diseases. *Cells* **2014**, *3*, 517–545. [[CrossRef](#)]
7. Gambino, G.; Rizzo, V.; Giglia, G.; Ferraro, G.; Sardo, P. Cannabinoids, TRPV and nitric oxide: The three ring circus of neuronal excitability. *Brain Struct. Funct.* **2020**, *225*, 1–15. [[CrossRef](#)]
8. Maione, S.; Starowicz, K.; Cristino, L.; Guida, F.; Palazzo, E.; Luongo, L.; Rossi, F.; Marabese, I.; de Novellis, V.; Di Marzo, V. Functional interaction between TRPV1 and μ -opioid receptors in the descending antinociceptive pathway activates glutamate transmission and induces analgesia. *J. Neurophysiol.* **2009**, *101*, 2411–2422. [[CrossRef](#)]
9. Morgan, M.M.; Whittier, K.L.; Hegarty, D.M.; Aicher, S.A. Periaqueductal gray neurons project to spinally projecting GABAergic neurons in the rostral ventromedial medulla. *Pain* **2008**, *140*, 376–386. [[CrossRef](#)]
10. Yanarates, O.; Dogrul, A.; Yildirim, V.; Sahin, A.; Sizlan, A.; Seyrek, M.; Akgül, Ö.; Kozak, O.; Kurt, E.; Aypar, U. Spinal 5-HT7 receptors play an important role in the antinociceptive and antihyperalgesic effects of tramadol and its metabolite, O-Desmethyltramadol, via activation of descending serotonergic pathways. *J. Am. Soc. Anesthesiol.* **2010**, *112*, 696–710. [[CrossRef](#)]
11. Holloway, B.B.; Stornetta, R.L.; Bochorishvili, G.; Erisir, A.; Viar, K.E.; Guyenet, P.G. Monosynaptic glutamatergic activation of locus coeruleus and other lower brainstem noradrenergic neurons by the C1 cells in mice. *J. Neurosci.* **2013**, *33*, 18792–18805. [[CrossRef](#)] [[PubMed](#)]
12. Brenchat, A.; Nadal, X.; Romero, L.; Ovalle, S.; Muro, A.; Sánchez-Arroyos, R.; Portillo-Salido, E.; Pujol, M.; Montero, A.; Codony, X. Pharmacological activation of 5-HT7 receptors reduces nerve injury-induced mechanical and thermal hypersensitivity. *Pain* **2010**, *149*, 483–494. [[CrossRef](#)] [[PubMed](#)]
13. Llorca-Torralba, M.; Borges, G.; Neto, F.; Mico, J.A.; Berrocoso, E. Noradrenergic Locus Coeruleus pathways in pain modulation. *Neuroscience* **2016**, *338*, 93–113. [[CrossRef](#)] [[PubMed](#)]
14. Hodgman, M.J.; Garrard, A.R. A review of acetaminophen poisoning. *Crit. Care Clin.* **2012**, *28*, 499–516. [[CrossRef](#)] [[PubMed](#)]
15. Ramachandran, A.; Jaeschke, H. Acetaminophen hepatotoxicity: A mitochondrial perspective. *Adv. Pharmacol.* **2019**, *85*, 195–219.
16. Marin, T.M.; de Carvalho Indolfo, N.; Rocco, S.A.; Basei, F.L.; de Carvalho, M.; de Almeida Gonçalves, K.; Pagani, E. Acetaminophen absorption and metabolism in an intestine/liver microphysiological system. *Chem. Biol. Interact.* **2019**, *299*, 59–76. [[CrossRef](#)]
17. McGill, M.R.; Jaeschke, H. Metabolism and disposition of acetaminophen: Recent advances in relation to hepatotoxicity and diagnosis. *Pharm. Res.* **2013**, *30*, 2174–2187. [[CrossRef](#)]
18. Graham, G.G.; Davies, M.J.; Day, R.O.; Mohamudally, A.; Scott, K.F. The modern pharmacology of paracetamol: Therapeutic actions, mechanism of action, metabolism, toxicity and recent pharmacological findings. *Inflammopharmacology* **2013**, *21*, 201–232. [[CrossRef](#)]
19. Barbier-Torres, L.; Iruzubieta, P.; Fernández-Ramos, D.; Delgado, T.C.; Taibo, D.; Guitierrez-de-Juan, V.; Varela-Rey, M.; Azkargorta, M.; Navasa, N.; Fernández-Tussy, P. The mitochondrial negative regulator MCL1 is a therapeutic target for acetaminophen-induced liver injury. *Nat. Commun.* **2017**, *8*, 2068. [[CrossRef](#)]
20. Stueber, T.; Meyer, S.; Jangra, A.; Hage, A.; Eberhardt, M.; Leffler, A. Activation of the capsaicin-receptor TRPV1 by the acetaminophen metabolite N-arachidonoylaminophenol results in cytotoxicity. *Life Sci.* **2018**, *194*, 67–74. [[CrossRef](#)]
21. Caballero, F.J.; Soler-Torronteras, R.; Lara-Chica, M.; García, V.; Fiebich, B.L.; Muñoz, E.; Calzado, M.A. AM404 inhibits NFAT and NF- κ B signaling pathways and impairs migration and invasiveness of neuroblastoma cells. *Eur. J. Pharmacol.* **2015**, *746*, 221–232. [[CrossRef](#)] [[PubMed](#)]
22. Sharma, C.V.; Long, J.H.; Shah, S.; Rahman, J.; Perrett, D.; Ayoub, S.S.; Mehta, V. First evidence of the conversion of paracetamol to AM404 in human cerebrospinal fluid. *J. Pain Res.* **2017**, *10*, 2703–2709. [[CrossRef](#)] [[PubMed](#)]
23. Högestätt, E.D.; Jönsson, B.A.; Ermund, A.; Andersson, D.A.; Björk, H.; Alexander, J.P.; Cravatt, B.F.; Basbaum, A.I.; Zygmunt, P.M. Conversion of acetaminophen to the bioactive N-acylphenolamine AM404 via fatty acid amide hydrolase-dependent arachidonic acid conjugation in the nervous system. *J. Biol. Chem.* **2005**, *280*, 31405–31412. [[CrossRef](#)]
24. Saliba, S.W.; Bonifacino, T.; Serchov, T.; Bonanno, G.; de Oliveira, A.C.P.; Fiebich, B.L. Neuroprotective effect of AM404 against NMDA-induced hippocampal excitotoxicity. *Front. Cell. Neurosci.* **2019**, *13*, 566. [[CrossRef](#)]
25. Abu Rmilah, A.; Zhou, W.; Nelson, E.; Lin, L.; Amiot, B.; Nyberg, S.L. Understanding the marvels behind liver regeneration. *Wiley Interdiscip. Rev. Dev. Biol.* **2019**, *8*, e340. [[CrossRef](#)]
26. Behari, J. The Wnt/ β -catenin signaling pathway in liver biology and disease. *Expert Rev. Gastroenterol. Hepatol.* **2010**, *4*, 745–756. [[CrossRef](#)] [[PubMed](#)]
27. Meng, Z.; Moroishi, T.; Guan, K.-L. Mechanisms of Hippo pathway regulation. *Genes Dev.* **2016**, *30*, 1–17. [[CrossRef](#)] [[PubMed](#)]
28. Park, H.W.; Kim, Y.C.; Yu, B.O.; Moroishi, T.; Mo, J.-S.; Plouffe, S.W.; Meng, Z.; Lin, K.C.; Yu, F.-X.; Alexander, C.M. Alternative Wnt signaling activates YAP/TAZ. *Cell* **2015**, *162*, 780–794. [[CrossRef](#)]
29. Elpek, G.Ö. Angiogenesis and liver fibrosis. *World J. Hepatol.* **2015**, *7*, 377. [[CrossRef](#)]

30. Ebrahem, Q.; Chaurasia, S.S.; Vasanji, A.; Qi, J.H.; Klenotic, P.A.; Cutler, A.; Asosingh, K.; Erzurum, S.; Anand-Apte, B. Cross-talk between vascular endothelial growth factor and matrix metalloproteinases in the induction of neovascularization in vivo. *Am. J. Pathol.* **2010**, *176*, 496–503. [[CrossRef](#)]
31. Norden, P.R.; Kim, D.J.; Barry, D.M.; Cleaver, O.B.; Davis, G.E. Cdc42 and k-Ras control endothelial tubulogenesis through apical membrane and cytoskeletal polarization: Novel stimulatory roles for GTPase effectors, the small GTPases, Rac2 and Rap1b, and inhibitory influence of Arhgap31 and Rasa1. *PLoS ONE* **2016**, *11*, e0147758. [[CrossRef](#)]
32. Hakanpaa, L.; Sipila, T.; Leppanen, V.-M.; Gautam, P.; Nurmi, H.; Jacquemet, G.; Eklund, L.; Ivaska, J.; Alitalo, K.; Saharinen, P. Endothelial destabilization by angiopoietin-2 via integrin β 1 activation. *Nat. Commun.* **2015**, *6*, 5962. [[CrossRef](#)] [[PubMed](#)]
33. Strazzabosco, M.; Fabris, L. Development of the bile ducts: Essentials for the clinical hepatologist. *J. Hepatol.* **2012**, *56*, 1159–1170. [[CrossRef](#)] [[PubMed](#)]
34. Soriano-Ursúa, M.A.; Das, B.C.; Trujillo-Ferrara, J.G. Boron-containing compounds: Chemico-biological properties and expanding medicinal potential in prevention, diagnosis and therapy. *Expert Opin. Ther. Pat.* **2014**, *24*, 485–500. [[CrossRef](#)]
35. Rosalez, M.N.; Estevez-Fregoso, E.; Alatorre, A.; Abad-García, A.; Soriano-Ursúa, M.A. 2-Aminoethyldiphenyl Borinate: A Multitarget Compound with Potential as a Drug Precursor. *Curr. Mol. Pharmacol.* **2020**, *13*, 57–75. [[CrossRef](#)] [[PubMed](#)]
36. Lorke, D. A new approach to practical acute toxicity testing. *Arch. Toxicol.* **1983**, *54*, 275–287. [[CrossRef](#)]
37. Kane, A.E.; Mitchell, S.J.; Mach, J.; Huizer-Pajkos, A.; McKenzie, C.; Jones, B.; Cogger, V.; Le Couteur, D.G.; de Cabo, R.; Hilmer, S.N. Acetaminophen hepatotoxicity in mice: Effect of age, frailty and exposure type. *Exp. Gerontol.* **2016**, *73*, 95–106. [[CrossRef](#)]
38. Lu, H.-H.; Thomas, J.D.; Tukker, J.J.; Fleisher, D. Intestinal water and solute absorption studies: Comparison of in situ perfusion with chronic isolated loops in rats. *Pharm. Res.* **1992**, *9*, 894–900. [[CrossRef](#)]
39. Ocampo-Néstor, A.L.; Trujillo-Ferrara, J.G.; Abad-García, A.; Reyes-López, C.; Geninatti-Crich, S.; Soriano-Ursua, M.A. Boron's journey: Advances in the study and application of pharmacokinetics. *Expert Opin. Ther. Pat.* **2017**, *27*, 203–215. [[CrossRef](#)]
40. Zhao, L.; Pickering, G. Paracetamol metabolism and related genetic differences. *Drug Metab. Rev.* **2011**, *43*, 41–52. [[CrossRef](#)]
41. Tjølsen, A.; Rosland, J.H.; Berge, O.-G.; Hole, K. The increasing-temperature hot-plate test: An improved test of nociception in mice and rats. *J. Pharmacol. Methods* **1991**, *25*, 241–250. [[CrossRef](#)] [[PubMed](#)]
42. Seibenhener, M.L.; Wooten, M.C. Use of the open field maze to measure locomotor and anxiety-like behavior in mice. *J. Vis. Exp. JoVE* **2015**, 52434. [[CrossRef](#)]
43. Maahs, D.M.; DeSalvo, D.; Pyle, L.; Ly, T.; Messer, L.; Clinton, P.; Westfall, E.; Wadwa, R.P.; Buckingham, B. Effect of acetaminophen on CGM glucose in an outpatient setting. *Diabetes Care* **2015**, *38*, e158–e159. [[CrossRef](#)]
44. Basu, A.; Veettil, S.; Dyer, R.; Peyser, T.; Basu, R. Direct evidence of acetaminophen interference with subcutaneous glucose sensing in humans: A pilot study. *Diabetes Technol. Ther.* **2016**, *18*, S2–S43. [[CrossRef](#)]
45. Donoiu, I.; Militaru, C.; Obleagă, O.; Hunter, J.M.; Neamțu, J.; Biță, A.; Scorei, I.R.; Rogoveanu, O.C. Effects of boron-containing compounds on cardiovascular disease risk factors—A review. *J. Trace Elem. Med. Biol.* **2018**, *50*, 47–56. [[CrossRef](#)]
46. López-Cabrera, Y.; Castillo-García, E.L.; Altamirano-Espino, J.A.; Pérez-Capistran, T.; Farfán-García, E.D.; Trujillo-Ferrara, J.G.; Soriano-Ursúa, M.A. Profile of three boron-containing compounds on the body weight, metabolism and inflammatory markers of diabetic rats. *J. Trace Elem. Med. Biol.* **2018**, *50*, 424–429. [[CrossRef](#)]
47. Keshet, R.; Szlosarek, P.; Carracedo, A.; Erez, A. Rewiring urea cycle metabolism in cancer to support anabolism. *Nat. Rev. Cancer* **2018**, *18*, 634–645. [[CrossRef](#)] [[PubMed](#)]
48. Kazak, L.; Cohen, P. Creatine metabolism: Energy homeostasis, immunity and cancer biology. *Nat. Rev. Endocrinol.* **2020**, *16*, 421–436. [[CrossRef](#)]
49. Syal, K.; Banerjee, D.; Srinivasan, A. Creatinine estimation and interference. *Indian J. Clin. Biochem.* **2013**, *28*, 210–211. [[CrossRef](#)]
50. Wyss, M.; Kaddurah-Daouk, R. Creatine and creatinine metabolism. *Physiol. Rev.* **2000**, *80*, 1107–1213. [[CrossRef](#)]
51. Estevez-Fregoso, E.; Kilic, A.; Rodríguez-Vera, D.; Nicanor-Juárez, L.E.; Romero-Rizo, C.E.M.; Farfán-García, E.D.; Soriano-Ursúa, M.A. Effects of Boron-Containing Compounds on Liposoluble Hormone Functions. *Inorganics* **2023**, *11*, 84. [[CrossRef](#)]
52. Röhrl, C.; Stangl, H. Cholesterol metabolism—Physiological regulation and pathophysiological deregulation by the endoplasmic reticulum. *Wien. Med. Wochenschr.* **2018**, *168*, 280. [[CrossRef](#)] [[PubMed](#)]
53. Özsoy, M.B.; Pabuçcuoğlu, A. The effect of acetaminophen on oxidative modification of low-density lipoproteins in hypercholesterolemic rabbits. *J. Clin. Biochem. Nutr.* **2007**, *41*, 27–31. [[CrossRef](#)] [[PubMed](#)]
54. Chou, T.; Greenspan, P. Effect of acetaminophen on the myeloperoxidase–hydrogen peroxide–nitrite mediated oxidation of LDL. *Biochim. Biophys. Acta (BBA)-Molecular Cell Biol. Lipids* **2002**, *1581*, 57–63. [[CrossRef](#)]
55. Herrington, W.; Illingworth, N.; Staplin, N.; Kumar, A.; Storey, B.; Hrusecka, R.; Judge, P.; Mahmood, M.; Parish, S.; Landray, M. Effect of processing delay and storage conditions on urine albumin-to-creatinine ratio. *Clin. J. Am. Soc. Nephrol.* **2016**, *11*, 1794–1801. [[CrossRef](#)]
56. Levitt, D.G.; Levitt, M.D. Human serum albumin homeostasis: A new look at the roles of synthesis, catabolism, renal and gastrointestinal excretion, and the clinical value of serum albumin measurements. *Int. J. Gen. Med.* **2016**, *9*, 229–255. [[CrossRef](#)] [[PubMed](#)]
57. Merlot, A.M.; Kalinowski, D.S.; Richardson, D.R. Unraveling the mysteries of serum albumin—More than just a serum protein. *Front. Physiol.* **2014**, *5*, 299. [[CrossRef](#)]
58. Ekam, V.S.; Udosen, E.O. Total protein, albumin and globulin levels following the administration of activity directed fractions of *Vernonia amygdalina* during acetaminophen induced hepatotoxicity in Wistar albino rats. *Glob. J. Pure Appl. Sci.* **2012**, *18*, 25–29.

59. Prinville, V.; Ohlund, L.; Sleno, L. Targeted analysis of 46 bile acids to study the effect of acetaminophen in rat by LC-MS/MS. *Metabolites* **2020**, *10*, 26. [[CrossRef](#)]
60. Al-Doaiss, A.A. Hepatotoxicity-Induced by the therapeutic dose of acetaminophen and the ameliorative effect of oral co-administration of selenium/Tribulus terrestris extract in rats. *Int. J. Morphol.* **2020**, *38*, 1444–1454. [[CrossRef](#)]
61. Manautou, J.E.; De Waart, D.R.; Kunne, C.; Zelcer, N.; Goedken, M.; Borst, P.; Elferink, R.O. Altered disposition of acetaminophen in mice with a disruption of the Mrp3 gene. *Hepatology* **2005**, *42*, 1091–1098. [[CrossRef](#)] [[PubMed](#)]
62. Zhou, J.; Tracy, T.S.; Rimmel, R.P. Bilirubin glucuronidation revisited: Proper assay conditions to estimate enzyme kinetics with recombinant UGT1A1. *Drug Metab. Dispos.* **2010**, *38*, 1907–1911. [[CrossRef](#)] [[PubMed](#)]
63. Tang, Z.; Chen, H.; He, H.; Ma, C. Assays for alkaline phosphatase activity: Progress and prospects. *TrAC Trends Anal. Chem.* **2019**, *113*, 32–43. [[CrossRef](#)]
64. Wicaksono, S.A.; Mardin, A.M.F.; Utami, S.B. The Effect of Paracetamol and Codeine Analgesic Combination on Serum Alanine Aminotransferase and Aspartate Aminotransferase Levels in Male Wistar Rats. *Open Access Maced. J. Med. Sci.* **2022**, *10*, 2267–2272. [[CrossRef](#)]
65. Çelik, M.; Aydin, P. Investigation of the effect of 4-hydroxyphenylboronic acid on acetaminophen-induced liver cell injury in HEPG2 cell line. *J. Boron* **2022**, *7*, 507–513. [[CrossRef](#)]
66. Nevzorova, Y.A.; Tolba, R.; Trautwein, C.; Liedtke, C. Partial hepatectomy in mice. *Lab. Anim.* **2015**, *49*, 81–88. [[CrossRef](#)]
67. Marongiu, F.; Marongiu, M.; Contini, A.; Serra, M.; Cadoni, E.; Murgia, R.; Laconi, E. Hyperplasia vs hypertrophy in tissue regeneration after extensive liver resection. *World J. Gastroenterol.* **2017**, *23*, 1764. [[CrossRef](#)]
68. Andersen, K.J.; Knudsen, A.R.; Kannerup, A.-S.; Sasanuma, H.; Nyengaard, J.R.; Hamilton-Dutoit, S.; Erlandsen, E.J.; Jørgensen, B.; Mortensen, F.V. The natural history of liver regeneration in rats: Description of an animal model for liver regeneration studies. *Int. J. Surg.* **2013**, *11*, 903–908. [[CrossRef](#)]
69. Kaware, M. Changes in liver and body weight of mice exposed to toxicant. *Int. J. Sci. Eng* **2013**, *3*, 92–95.
70. Böhm, F.; Köhler, U.A.; Speicher, T.; Werner, S. Regulation of liver regeneration by growth factors and cytokines. *EMBO Mol. Med.* **2010**, *2*, 294–305. [[CrossRef](#)]
71. Li, J.-X.; Fei, X.-M.; Lu, H.; Hu, H.-J.; Li, J.-Y. Effect of proteasome inhibitor on migration ability and hepatocyte growth factor expression of bone marrow mesenchymal stem cells in multiple myeloma patients. *Zhongguo Shi Yan Xue Ye Xue Za Zhi* **2011**, *19*, 1204–1208. [[PubMed](#)]
72. Tee, L.B.G.; Davies, D.S.; Seddon, C.E.; Boobis, A.R. Species differences in the hepatotoxicity of paracetamol are due to differences in the rate of conversion to its cytotoxic metabolite. *Biochem. Pharmacol.* **1987**, *36*, 1041–1052. [[CrossRef](#)] [[PubMed](#)]
73. Dickinson, A.L.; Leach, M.C.; Flecknell, P.A. The analgesic effects of oral paracetamol in two strains of mice undergoing vasectomy. *Lab. Anim.* **2009**, *43*, 357–361. [[CrossRef](#)]
74. Gao, Y.; Cao, E.; Julius, D.; Cheng, Y. TRPV1 structures in nanodiscs reveal mechanisms of ligand and lipid action. *Nature* **2016**, *534*, 347–351. [[CrossRef](#)] [[PubMed](#)]
75. Soriano-Ursúa, M.A.; Bello, M.; Hernández-Martínez, C.F.; Santillán-Torres, I.; Guerrero-Ramírez, R.; Correa-Basurto, J.; Arias-Montaño, J.A.; Trujillo-Ferrara, J.G. Cell-based assays and molecular dynamics analysis of a boron-containing agonist with different profiles of binding to human and guinea pig beta2 adrenoceptors. *Eur. Biophys. J.* **2019**, *48*, 83–97. [[CrossRef](#)]
76. Farfán-García, E.D.; Rosales-Hernández, M.C.; Castillo-García, E.L.; Abad-García, A.; Ruiz-Maciel, O.; Velasco-Silveyra, L.M.; González-Muñoz, A.Y.; Andrade-Jorge, E.; Soriano-Ursúa, M.A. Identification and evaluation of boronic compounds ameliorating cognitive deficit in orchiectomized rats. *J. Trace Elem. Med. Biol.* **2022**, *72*, 126979. [[CrossRef](#)]
77. Morris, G.M.; Huey, R.; Lindstrom, W.; Sanner, M.F.; Belew, R.K.; Goodsell, D.S.; Olson, A.J. AutoDock4 and AutoDockTools4: Automated docking with selective receptor flexibility. *J. Comput. Chem.* **2009**, *30*, 2785–2791. [[CrossRef](#)]
78. Popov, I.A.; Boldyrev, A.I. Classical and Multicenter Bonding in Boron: Two Faces of Boron. In *Boron. Challenges and Advances in Computational Chemistry and Physics*; Hnyk, D., McKee, M., Eds.; Springer: Cham, Switzerland, 2015; Volume 20, pp. 1–16. [[CrossRef](#)]
79. Chinedu, E.; Arome, D.; Solomon Ameh, F. A new method for determining acute toxicity in animal models. *Toxicol. Int.* **2013**, *20*, 224–226. [[CrossRef](#)]
80. Higgins, G. Experimental pathology of the liver. Restoration of the liver of the white rat following partial surgical removal. *AMA Arch Pathol* **1931**, *12*, 186–202.
81. Madrigal-Santillán, E.; Bautista, M.; Gayosso-De-Lucio, J.A.; Reyes-Rosales, Y.; Posadas-Mondragón, A.; Morales-González, Á.; Soriano-Ursúa, M.A.; García-Machorro, J.; Madrigal-Bujaidar, E.; Álvarez-González, I.; et al. Hepatoprotective effect of *Geranium schiedeanum* against ethanol toxicity during liver regeneration. *World J. Gastroenterol.* **2015**, *21*, 7718. [[CrossRef](#)]

Disclaimer/Publisher’s Note: The statements, opinions and data contained in all publications are solely those of the individual author(s) and contributor(s) and not of MDPI and/or the editor(s). MDPI and/or the editor(s) disclaim responsibility for any injury to people or property resulting from any ideas, methods, instructions or products referred to in the content.